Hindawi
International Journal of Aerospace Engineering
Volume 2022, Article ID 1637305, 11 pages
https://doi.org/10.1155/2022/1637305

Research Article

Fault-Tolerant Control of Hypersonic Vehicle Using Neural Network and Sliding Mode

Peng Cui, Changsheng Gao, Wuxing Jing, and Ruoming An

School of Astronautics, Harbin Institute of Technology, Harbin 150001, China

Correspondence should be addressed to Ruoming An; anruoming@hit.edu.com

Received 31 March 2022; Revised 29 July 2022; Accepted 16 September 2022; Published 11 October 2022

Academic Editor: Youmin Zhang

In this paper, the tracking control of the air-breathing hypersonic vehicle with model parameter uncertainties and actuator faults is studied. Firstly, a high-order linearization model is used to build an adaptive terminal sliding mode that eliminates chattering and provides increased robustness for unknown disturbances in the system. Second, a fault-tolerant control method mixing the radial basis function neural network with adaptive sliding mode control is suggested, with the addition of a hyperbolic tangent function to avoid controller input saturation. Finally, the stability of the controller is proved strictly by the Lyapunov theory, and the robustness and effectiveness of the controller are further verified by numerical simulations of the longitudinal model of the hypersonic vehicle.

1. Introduction

Air-breathing hypersonic vehicles (ABHV) are an appealing technology for military and low-cost space access needs. The aerodynamic properties of ABHV make flight control more susceptible to parameter errors and actuator faults than traditional flying aircraft at high attitude and Mach numbers. Strong fault-tolerant control systems should therefore be created for ABHVs to guarantee flight safety [1]. Various researchers have been researching hypersonic vehicle modelling since the 1990s, which is used to describe the dynamic characteristics of hypersonic vehicles. Marrison and Stengel suggested a high-fidelity longitudinal dynamics model based on the universal hypersonic vehicle developed at NASA Langley Research Center [2]. Strong nonlinear, time-varying, and nonminimum phase characteristics are the main features of a hypersonic vehicle. The longitudinal dynamics of ABHV are linearized to higher order [3]. Many sophisticated control techniques [4], including adaptive control [5], backstepping control [6], predictive control [7], fuzzy control [8], and feedback linearization control [9], can be employed to form fault-tolerant controllers for ABHV.

Sliding mode control is one of the most appealing nonlinear control tools among all types of control approaches. The feedback linearization model is used to construct an adaptive sliding mode controller with model uncertainty [10]. Because the linear sliding mode surface can only converge exponentially, the integral sliding mode controller is employed to achieve finite-time state convergence [11]. Based on this finite-time integral sliding mode surface, a simplified smooth second-order sliding mode approach law can realize synchronous convergence to zero [12]. In addition, finite-time convergence of states can be realized by terminal sliding mode, and unknown actuator faults can be estimated by adaptive law [13]. In the meantime, the sliding mode observer (SMO) may be used to assess actuator fault information and model uncertainty, and the estimation error converges in a finite amount of time [14] .

In actuality, system uncertainty and actuator faults are difficult to model. For dynamics that cannot be modeled, neural networks have been shown to be able to approximate any continuous function [15]. The typical way is always to build the feedback controller according to the model and then use the neural network to estimate the system disturbance to adjust the control input [16] . It is easy to convert model parameter uncertainties into system disturbances using neural network compensation to increase the robustness of the feedback controller [17]. In some cases [18],

neural networks may approximate the model function and gain function for a nonlinear system, hence increasing robustness [19]. Further, the control input may be defined as a new object function [20], and a radial basis function neural network may also be employed to approximate it. As a result, the uncertainty induced by actuator failure may be predicted using a neural network [21, 22].

Despite substantial advances in fault-tolerant hypersonic vehicle management, the accompanying literature analysis demonstrates that there is still room for improvement [23, 24]. For example, just the actuator failure was analyzed, ignoring bias and outage failures. Although the failure observer's assistance was used to estimate failure information, the overall system's stability was not revealed, making it impossible to assess the process's condition at any time. We investigate the failure tracking control of a hypersonic vehicle employing terminal sliding mode theory and a neural network approach in this research [25–29]. In this paper, a fault-tolerant control (FTC) method combining radial basis function neural network (RBFNN) and adaptive terminal sliding mode (ATSM) is proposed, which can track the ABHV trajectory of an ABHV in the presence of air density, mass, and moment of inertia uncertainties as well as actuator faults. The main contributions of this paper are as follows:

(1) This scheme resolves the coupling problem in MIMO systems like ABHV, which has theoretical implications

(2) The RBFNN may approximate the actuator's fault characteristics and provide the hyperbolic tangent function to prevent saturation of the control input, thus assuring the control system's practical application value

(3) This fault-tolerant control scheme ensures the ABHV closed-loop control system's stability and allows for a fast and effective reaction to the reference trajectory

The arrangement of this paper is as follows:

In Section 2, the longitudinal dynamics model of ABHV is input and output linearized, as well as actuator fault modelling and control input antisaturation processing. Then, Section 3 introduces the prior knowledge of RBFNN and the relevant lemma needed for controller design. The FTC scheme based on RBFNN is designed for the control model in Section 2. In Section 4, the ABHV model with and without faults is numerically simulated. Finally, this paper is summarised in Section 5.

2. Problem Statements

The longitudinal model of the ABHV is described as follows [8]:

$$\begin{aligned}
\dot{V} &= \frac{T\cos\alpha - D}{m} - g\sin\gamma,\\
\dot{h} &= V\sin\gamma,\\
\dot{\gamma} &= \frac{L + T\sin\alpha}{mV} - \left(\frac{g}{V} - \frac{V}{r}\right)\cos\gamma,\\
\dot{\alpha} &= q - \dot{\gamma},\\
\dot{q} &= \frac{M_y}{I_{yy}},
\end{aligned} \tag{1}$$

where V is the flight velocity, α is the angle of attack, h is the flight altitude, γ is the flight path angle (FPA), and q is the pitch rate. I_{yy} is the moment of inertia, m is the ABHV's mass, $g = \mu/(R_e + h)^2$ is the gravitational acceleration, and R_e is the earth's radius. L is the lift force, T is the thrust of engine, D is the resistance, and M is the pitching moment. These forces, torques, and coefficients of ABHV are as follows:

$$\begin{aligned}
&L = 0.5\rho V^2 S C_L,\ \mathrm{C}_L = 0.6203\alpha,\\
&D = 0.5\rho V^2 S C_D,\ C_D = 0.6450\alpha^2 + 0.0043378\alpha + 0.003772,\\
&T = 0.5\rho V^2 S C_T,\\
&C_T = \begin{cases} 0.02576\phi, & \phi < 1,\\ 0.0224 + 0.00336\phi, & \phi \geq 1,\end{cases}\\
&M = 0.5\rho V^2 S\bar{c} C_M,\ C_M = C_M(\alpha) + C_M(q) + C_M(\delta),\\
&C_M(\alpha) = -0.035\alpha^2 + 0.036617\alpha + 5.3261 \times 10^{-6},\\
&C_M(q) = \frac{\bar{c}}{2V} q\left(-6.796\alpha^2 + 0.3015\alpha - 0.2289\right),\\
&C_M(\delta) = 0.0292(\delta_e - \alpha),
\end{aligned} \tag{2}$$

where δ_e is the elevator angular deflection and ϕ is fuel-to-air ratio. In fact, the actuator output is bounded and can be expressed as $\phi \in [\phi_{\min}, \phi_{\max}]$ and $\delta_e \in [\delta_{\min}, \delta_{\max}]$, where $\phi_{\min}$, $\phi_{\max}$, $\delta_{\min}$, and $\delta_{\max}$ are known constants. A second-order system describes the dynamics of the engine [11]:

$$\ddot{\phi} = -2\zeta\omega_n\dot{\phi} - \omega_n^2\phi + \omega_n^2\phi_c, \tag{3}$$

where ϕ_c signifies the control input demand, ω_n means the engine dynamics' natural frequency undamped, and ζ is the damping ratio. Because the control input is bound by Equation (4), the following hyperbolic tangent function is used to avoid control input saturation:

$$\begin{aligned}
\phi_L &= \frac{|\phi_{\min} - \phi_{\max}|}{2}\tanh\left(\frac{2\phi_c - (\phi_{\min} + \phi_{\max})}{|\phi_{\min} - \phi_{\max}|}\right),\\
\delta_L &= \frac{|\delta_{\min} - \delta_{\max}|}{2}\tanh\left(\frac{2\delta_e - (\delta_{\min} + \delta_{\max})}{|\delta_{\min} - \delta_{\max}|}\right).
\end{aligned} \tag{4}$$

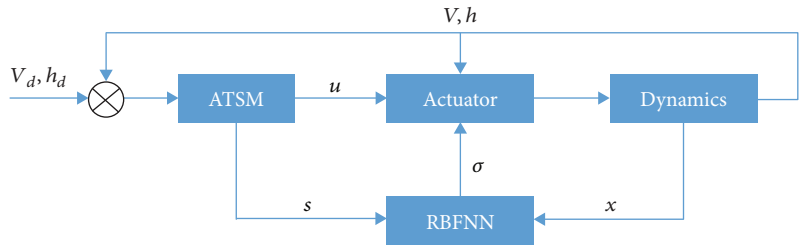

Figure 1: Control scheme.

Actuator faults can generally be described as a linear model:

$$u_F = k_F u_L + d_F, \tag{5}$$

where u_F is the control signals under faults, $u_L = [\phi_L \quad \delta_L]^T$ is the saturation input, $k_F = \text{diag}\,(k_{F_1} \quad k_{F_2})$ is the fault gain matrix, and $d_F = [d_{F_1} \quad d_{F_2}]^T$ is the vector of fault deviation.

3. Controller Design

Lemma 1 (approximation based on RBFNN). *The following RBFNNs can estimate an unknown smooth nonlinear function $f(x)$ on a compact set:*

$$f(x) = W^{*T} h(x) + \varepsilon, \tag{6}$$

where x is the input of network, W^{*T} is the ideal weight matrix, $h(x)$ is the convolution vector, and ε is the approximation error. $h(x) = [h_1 h_2 \cdots h_l]^T$ is chosen as the convolution formula:

$$h_j(x) = \exp\left(\frac{\|x - c_j\|^2}{2b_j^2}\right), \quad j = 1, 2, \cdots l, \tag{7}$$

where c_j and b_j are the center and width of the j-th neuron, respectively, and l is the node number of the neural networks.

In Figure 1, the FTC scheme framework combining RBFNN and ATSM proposed in this paper is shown.

In order to track ABHV's reference velocity V_d and reference altitude h_d, the state variable is set to $x = [V \quad \gamma \quad \alpha \quad q \quad \phi \quad \dot{\phi} \quad h]^T$, the input variable to $u = [\delta_e \phi_c]^T$, and the output variable to $y = [V \quad h]^T$. The tracking errors can be defined as $e_V = V - V_d$ and $e_h = h - h_d$.

The high-order linearization model of ABHV is shown as follows:

$$\begin{bmatrix} V^{(3)} \\ h^{(4)} \end{bmatrix} = \begin{bmatrix} f_V \\ f_h \end{bmatrix} + \begin{bmatrix} b_{11} & b_{12} \\ b_{21} & b_{22} \end{bmatrix} \begin{bmatrix} \phi_c \\ \delta_e \end{bmatrix}, \tag{8}$$

where f_V, f_h, b_{11}, b_{12}, b_{21}, and b_{22} are defined in [11]. The auxiliary variables [13] are introduced as

$$\begin{aligned} e_1 &= \begin{bmatrix} e_V + \dot{e}_V \\ e_h + \dot{e}_h + \ddot{e}_h \end{bmatrix}, \\ e_2 = \dot{e}_1 &= \begin{bmatrix} \dot{e}_V + \ddot{e}_V \\ \dot{e}_h + \ddot{e}_h + \dddot{e}_h \end{bmatrix}. \end{aligned} \tag{9}$$

Considering the influence of parameter uncertainty and external disturbance, the system can be defined as follows:

$$\begin{aligned} \dot{e}_1 &= e_2, \\ \dot{e}_2 &= f(x) + g(x)u + d, \end{aligned} \tag{10}$$

where $f(x)$, $g(x)$, and d are known in [13] as follows:

$$\begin{aligned} f(x) &= \begin{pmatrix} V_d^{(3)} \\ h_d^{(4)} \end{pmatrix} - \begin{pmatrix} f_V(x) \\ f_h(x) \end{pmatrix} + e_2(x) - \begin{pmatrix} \dot{e}_V(x) \\ \dot{e}_h(x) \end{pmatrix}, \\ g(x) &= \begin{bmatrix} b_{11} & b_{12} \\ b_{21} & b_{22} \end{bmatrix}, \\ d &= \begin{bmatrix} d_1 \\ d_2 \end{bmatrix}, \\ u &= \begin{bmatrix} \varphi_c \\ \delta_e \end{bmatrix}. \end{aligned} \tag{11}$$

Assumption 2. There exists a positive value d_u with an unknown upper bound, such that the system disturbance d satisfies:

$$\|d\|_\infty \le d_u. \tag{12}$$

Because the state variables and aerodynamic parameters are practically bounded, the disturbance d is a function of them and has a certain range of values.

In order to satisfy Lemma 1, a terminal sliding manifold is chosen as follows:

$$\begin{aligned} s &= e_2 + k_a e_1 + k_b P\left(e_1, \frac{q}{p}\right), \\ P\left(e_1, \frac{q}{p}\right) &= \left[\text{sign}\left(e_1^1\right)\left|e_1^1\right|^{q/p} \quad \text{sign}\left(e_1^2\right)\left|e_1^2\right|^{q/p}\right]^T, \end{aligned} \tag{13}$$

where $s = [s_1 \quad s_2]^T$, $e_1 = [e_1^1 \quad e_1^2]^T$, $e_2 = [e_2^1 \quad e_2^2]^T$, k_a, and k_b are positive constants. When q and p are positive odd numbers, and $p > q$, the sliding mode is Hurwitz.

The law of the sliding mode approach is as follows:

$$\dot{s} = -k_1[\text{sign}\,(s_1) \quad \text{sign}\,(s_2)]^T - k_2 s, \tag{14}$$

where k_1 and k_2 are positive constants.

Since the system disturbance d cannot be accurately obtained, a robust term $\widehat{d}$ is introduced in the form of

$$\widehat{d} = \widehat{d}_u^2 s + \frac{1}{4}\lambda_1^2 s, \tag{15}$$

where $\widehat{d}_u$ is the estimated value of d_u and λ_1 is a positive constant. The estimated error of d_u is defined as $\tilde{d}_u = d_u - \widehat{d}_u$.

Considering system (13), create a Lyapunov function by following these steps:

$$L_1 = \frac{1}{2}s^T s + \frac{1}{2}\tilde{d}_u^2. \tag{16}$$

The derivative of L_1 can be obtained:

$$\begin{aligned} \dot{L}_1 &= s^T \dot{s} + \tilde{d}_u \dot{\tilde{d}}_u \\ &= s^T\left(f(x) + g(x)u + d + k_a e_2 + k_b \dot{P}\left(e_1, \frac{q}{p}\right)\right) \\ &\quad - \tilde{d}_u \dot{\tilde{d}}_u, \end{aligned}$$

$$\dot{P}\left[\left(e_1, \frac{q}{p}\right) = \frac{q}{p}\,\text{sign}\left(e_1^1\right)\left|e_1^1\right|^{(q/p)-1} e_2^1 \;\text{sign}\left(e_1^2\right)\left|e_1^1\right|^{(q/p)-1} e_2^2\right]^T. \tag{17}$$

Applying Assumption 2 and the approach law (14), the ATSM system's input is constructed as follows:

$$\begin{aligned} u_s = g^{-1}\Big(&-f - \widehat{d} - k_a e_2 - k_b \dot{P}\left(e_1, \frac{q}{p}\right) \\ &- k_1[\text{sign}\,(s_1)\;\text{sign}\,(s_2)]^T - k_2 s\Big). \end{aligned} \tag{18}$$

By substituting the derivative from Equation (18) into Equation (17), the following may be deduced:

$$\dot{L}_1 \le -k_1\|s\|_1 - k_2 s^T s + \|d_u s\|_1 - s^T\left(\widehat{d}_u^2 s + \frac{1}{4}\lambda_1^2 s\right) - \tilde{d}_u \dot{\widehat{d}}_u. \tag{19}$$

The adaptive law of parameters $\widehat{d}_u$ is chosen as

$$\dot{\widehat{d}}_u = \lambda_1^2 s^T s - \lambda_2 \widehat{d}_u, \tag{20}$$

where λ_2 is positive constant.

Substituting Equation (20) into Equation (19), the following inequality relation can be obtained:

$$\|d_u s\|_1 - \widehat{d}_u^2 s^T s - \frac{1}{4}\lambda_1^2 s^T s - \tilde{d}_u \lambda_1^2 s^T s \le \frac{d_u}{4\lambda_1}. \tag{21}$$

Therefore, Equation (19) can be simplified as

$$\begin{aligned} \dot{L}_1 &\le -k_1\|s\|_1 - k_2 s^T s + \frac{d_u}{4\lambda_1} - \frac{1}{2}\lambda_2\tilde{d}_u^2 + \frac{1}{2}\lambda_2 d_u^2 - \frac{1}{2}\lambda_2\tilde{d}_u^2 \\ &\le -k_2 s^T s - \frac{1}{2}\lambda_2\tilde{d}_u^2 + \frac{d_u}{4\lambda_1} + \frac{1}{2}\lambda_2 d_u^2 \\ &\le -\min\left\{k_2, \frac{1}{2}\lambda_2\right\}L_1 + \frac{d_u}{4\lambda_1} + \frac{1}{2}\lambda_2 d_u^2. \end{aligned} \tag{22}$$

Taking into account the actuator faults and saturations, the system (10) can be represented as follows:

$$\begin{aligned} \dot{e}_1 &= e_2, \\ \dot{e}_2 &= f(x) + g(x)(u - \sigma(x)) + d, \end{aligned} \tag{23}$$

where $\sigma(x) = u - u_F$ are the errors between the control inputs and the control signals under faults.

The RBFNN is used to estimate $\sigma(x)$ the disturbance term given by the following:

$$\sigma = W^{*T} h(x) + \varepsilon. \tag{24}$$

The estimate error of σ can be described as

$$\tilde{\sigma} = \sigma - \widehat{\sigma} = \tilde{W}^T h + \varepsilon, \tag{25}$$

where $\widehat{W}$ is the estimate value of W^* and $\tilde{W} = W^* - \widehat{W}$ is the estimated error.

Assumption 3. The approximation error ε is supposed to be bound by an unknown positive constant ε_0 as follows:

$$\|\varepsilon\|_\infty \le \varepsilon_0. \tag{26}$$

According to Equation (18), the actual input of the FTC scheme is constructed as follows:

$$u = g^{-1}\left(-f - \widehat{d}_u^T \widehat{d}_u s - \frac{1}{4}\lambda_1^2 s - k_a e_2 - k_b \dot{P}\left(e_1, \frac{q}{p}\right) - k_1[\text{sign}\ (s_1) \quad \text{sign}\ (s_2)]^T - k_2 s\right) + \widehat{W}^T h(x). \tag{27}$$

For the system (23), the Lyapunov function L_2 corresponding to Equation (16) is created:

$$L_2 = L_1 + \frac{1}{2} tr\left(\tilde{W}^T \Gamma^{-1} \tilde{W}\right). \tag{28}$$

The derivative of L_2 can be found as follows:

$$\dot{L}_1 = s^T \dot{s} - \tilde{d}_u \dot{\tilde{d}}_u - tr\left(\tilde{W}^T \Gamma^{-1} \dot{\widehat{W}}\right). \tag{29}$$

Applying Equations (20), (23), and (27), the time derivative of L_3 can be written as

$$\dot{L}_2 \le -k_1 \|s\|_1 - k_2 s^T s - \frac{1}{2}\lambda_2 \tilde{d}_u^2 + \frac{d_u}{4\lambda_1} + \frac{1}{2}\lambda_2 d_u^2 - s^T g \tilde{W}^T h - s^T g\varepsilon - tr\left(\tilde{W}^T \Gamma^{-1} \dot{\widehat{W}}\right). \tag{30}$$

The adaptive adjustment law for $\widehat{W}$ is chosen as follows:

$$\dot{\widehat{W}} = -\Gamma\left(h s^T g + \lambda_3 \widehat{W}\right), \tag{31}$$

where λ_3 is a positive constant and Γ is a diagonal positive matrix.

Substituting Equation (31) into Equation (30), the time derivative of L_3 can be written as

$$\dot{L}_2 \le -k_1 \|s\|_1 - k_2 s^T s - \frac{1}{2}\lambda_2 \tilde{d}_u^2 + \frac{d_u}{4\lambda_1} + \frac{1}{2}\lambda_2 d_u^2 - s^T g \tilde{W}^T h - s^T g\varepsilon - tr\left(\tilde{W}^T h s^T g + \lambda_3 \tilde{W}^T \widehat{W}\right). \tag{32}$$

When $k_1 > \|\varepsilon_0^T g\|_\infty$, Equation (32) can be rewritten as:

$$\dot{L}_2 \le -k_1 \|s\|_1 - k_2 s^T s - \frac{1}{2}\lambda_2 \tilde{d}_u^2 + \frac{d_u}{4\lambda_1} + \frac{1}{2}\lambda_2 d_u^2 + \lambda_3 tr\left(\tilde{W}^T \widehat{W}\right). \tag{33}$$

According to the unequal relationship,

$$\begin{aligned} 2\tilde{W}^T \tilde{W} &= \tilde{W}^T\left(W^* - \widehat{W}\right) + \left(W^* - \widehat{W}\right)^T W \\ &= \tilde{W}^T W^* - \tilde{W}^T \tilde{W} + \widehat{W}^T W^* - \widehat{W}^T \widehat{W} \\ &= W^{*T} W^* - \tilde{W}^T \tilde{W} - \widehat{W}^T \widehat{W}, \\ tr\left(\tilde{W}^T \widehat{W}\right) &= \|W^*\|_2 - \left\|\tilde{W}\right\|_2 - \left\|\widehat{W}\right\|_2 \\ &\le \frac{1}{2}\left(\|W^*\|_2 - \left\|\tilde{W}\right\|_2\right). \end{aligned} \tag{34}$$

Substitute into Equation (32) to obtain

$$\dot{L}_2 \le -k_2 s^T s - \frac{1}{2}\lambda_2 \tilde{d}_u^2 - \frac{1}{2}\lambda_3 \left\|\tilde{W}\right\|_2 + \frac{d_u}{4\lambda_1} + \frac{1}{2}\lambda_2 d_u^2 + \frac{1}{2}\lambda_3 \|W^*\|_2. \tag{35}$$

When λ_4 is the largest eigenvalue of the matrix Γ^{-1}, $tr(\tilde{W}^T \Gamma^{-1} \tilde{W}) \le \lambda_4 \|\tilde{W}\|_2$, the following relationships exist:

$$\dot{L}_2 \le -k_L L_2 + \Delta, \tag{36}$$

where $k_L = \min\{k_2, (1/2)\lambda_2, \lambda_3/\lambda_4\}$ and $\Delta = (d_u/4\lambda) + ((1/2)\lambda_2 \|d_u\|^2) + ((1/2)\lambda_3 \|W^*\|^2)$.

The solution to formula (35) is as follows:

$$L_2(t) \le L_2(0) e^{-k_L t} + \frac{\Delta}{k_L} \le L_2(0) + \frac{\Delta}{k_L} \quad \forall t \ge 0. \tag{37}$$

According to Equations (22) and (37), it can be seen that all signals in the closed-loop control system are bounded. The state tracking errors e_V, e_h, e_1, and e_2, as well as the estimation errors of the disturbance's upper bound d_u and the neural network weights W^*, are bounded. Based on Lyapunov theory, the stability of this closed-loop system is uniformly ultimately stable and exponentially converge to a bounded neighbourhood of the system original point.

4. Simulation Results

In order to verify the effectiveness of the proposed control strategy, according to the dynamics models of Equations (1), (2), and (3), and by referring to the parameters of reference [2], simulation is carried out to make the aircraft track the given altitude command and speed command. The initial values of the states are set as $V_0 = 15060$ft/s, $h = 110000$ft, $\gamma = 0$rad, $\alpha = 0.0312$rad, $\phi = 0.1802$, $\dot{\phi} = 0$, and $q = 0$rad/s. The step command is $V_d = 15160$ft/s and $h_c = 112000$ft. The reference commands of V_r and h_r are calculated as follows:

$$\begin{aligned} \dot{x}_i &= x_{i+1} (i = 1, 2, \cdots, n-1), \\ \dot{x}_n &= \lambda^n x_d - \left(\frac{d}{dt} + \lambda\right)^n x_1, \end{aligned} \tag{38}$$

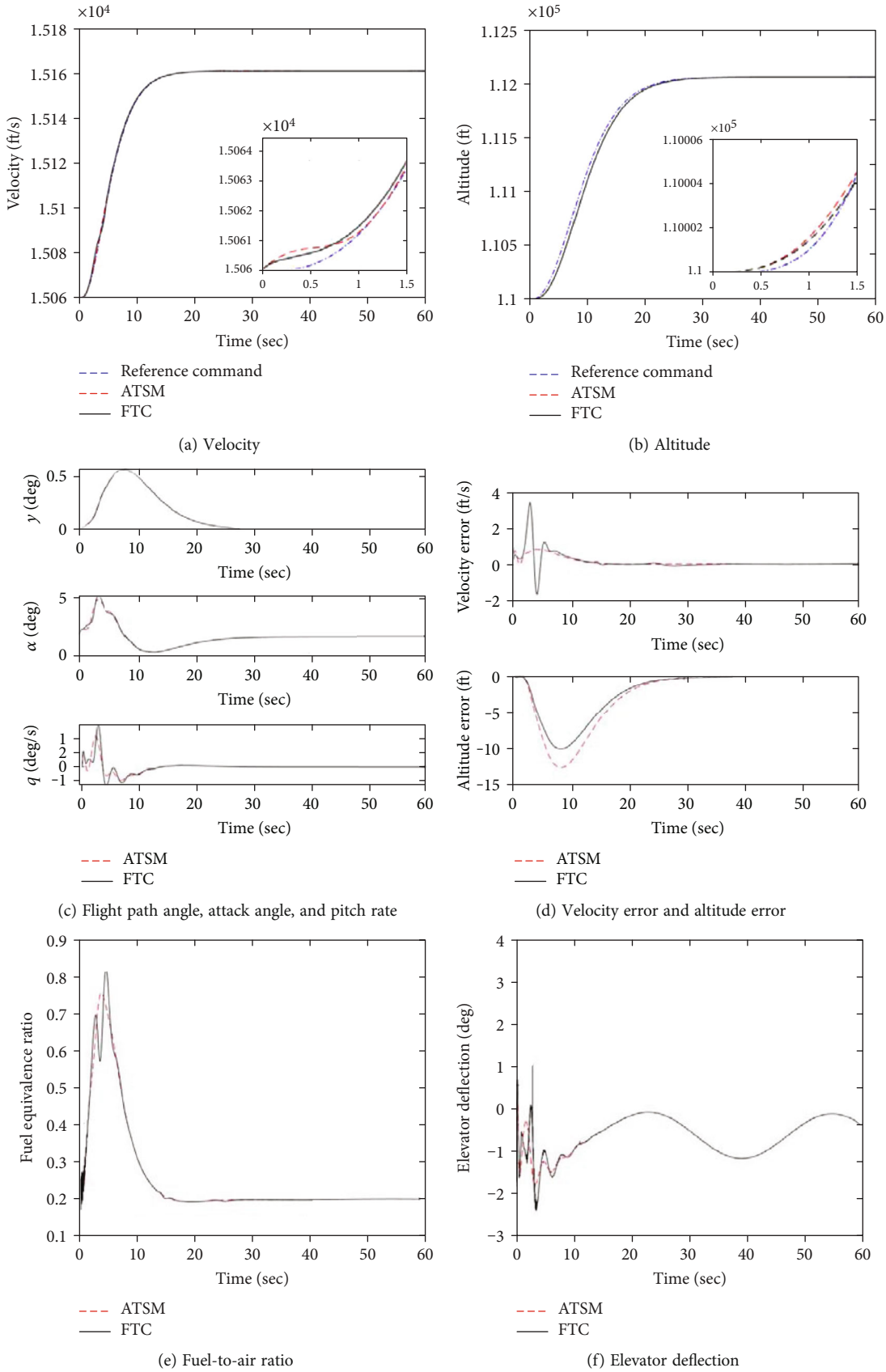

Figure 2: Continued.

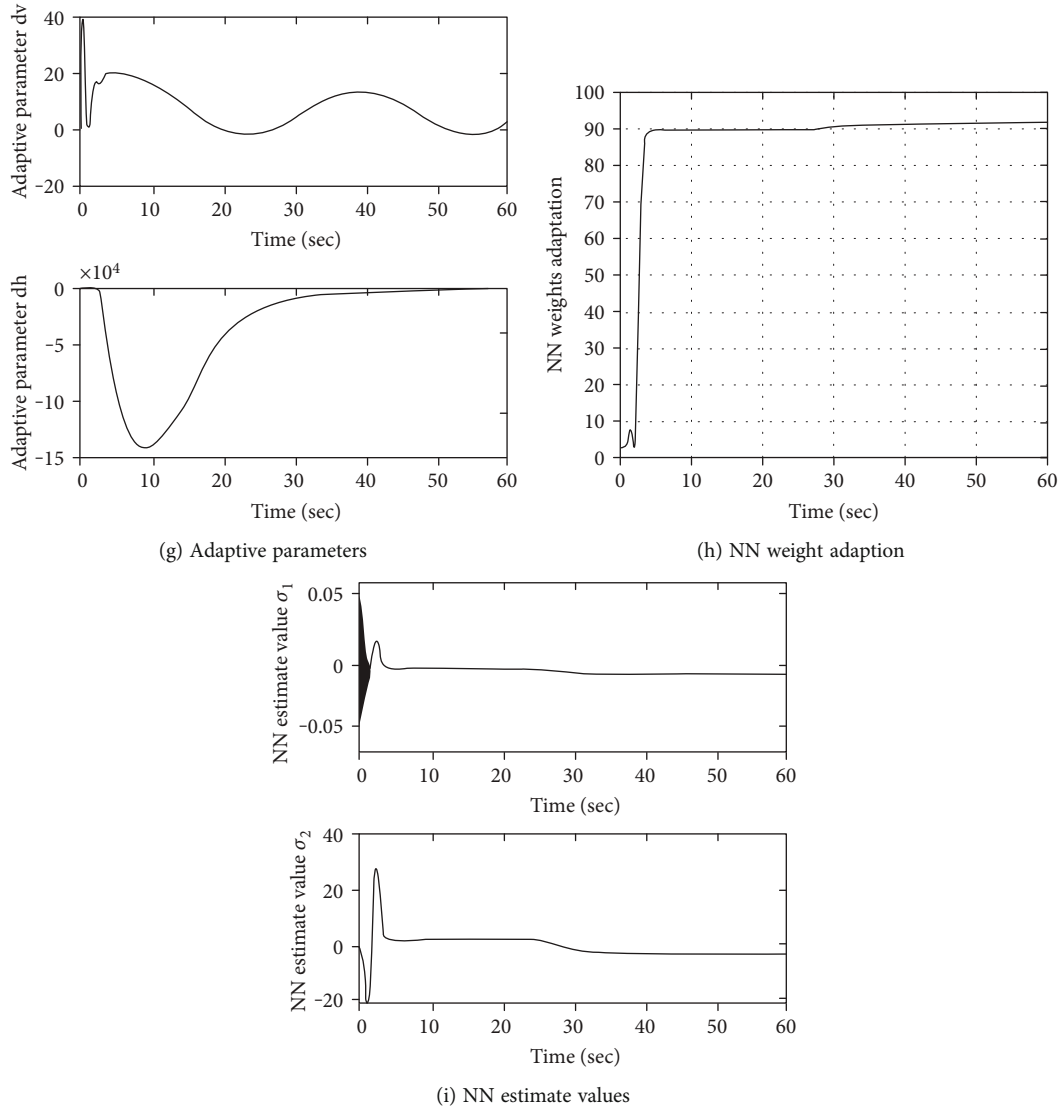

(g) Adaptive parameters

(h) NN weight adaption

(i) NN estimate values

Figure 2: Response curves of the ABHV's variables without the actuator faults.

with $\lambda_V = 0.5$ and $\lambda_h = 0.3$. To verify the robustness of the controller, the model parameters are processed as follows: $\Delta m = -0.03$, $\Delta I_{yy} = -0.03$, $\Delta \bar{c} = 0.03$, $\Delta c_{e0} = 0.03$, $\Delta \rho_0 = 0.03$, and $\Delta S_0 = 0.03$. The external disturbances [11–13] are given as $d_1 = 0.002 \sin(0.1t)$ and $d_2 = 0.01 \sin(0.2t)$.

The design parameters of the ATSM controller method in this paper are, respectively, set as $k_\alpha = 5$, $k_b = 0.01$, $p = 3$, $q = 1$, $k_1 = 5$, $k_2 = 10$, $\lambda_1 = 1.5$, $\lambda_2 = 0.02$, and $\lambda_3 = 0.01$. The design parameters of the FTC method in this paper are, respectively, set as $k_\alpha = 3$, $k_b = 0.1$, $p = 3$, $q = 1$, $k_1 = 10$, $k_2 = 10$, $\lambda_1 = 1.5$, $\lambda_2 = 0.02$, $\lambda_3 = 0.01$ $\widehat{W}_0 = 0_{11\times 2}$, $\Gamma = 200$ $I_{11\times 11}$, and $b_j = 100$.

The center value matrix $C = [C_1 C_2 \cdots C_{11}]$ of the Gaussian basis function is chosen as

$$C_{5\times 11} = [\,\mathrm{A}_{5\times 6} \quad \mathrm{B}_{5\times 5}\,],$$

$$\mathrm{A}_{5\times 6} = \begin{bmatrix} 14000 & 14200 & 14400 & 14600 & 14800 & 15000 \\ -0.0175 & -0.0140 & -0.0105 & -0.0070 & -0.0035 & 0 \\ -0.0873 & -0.0698 & -0.0524 & -0.0349 & -0.0175 & 0 \\ 0 & 0.1000 & 0.2000 & 0.3000 & 0.4000 & 0.5000 \\ 100000 & 102000 & 104000 & 106000 & 108000 & 110000 \end{bmatrix},$$

$$\mathrm{B}_{5\times 5} = \begin{bmatrix} 15200 & 15400 & 15600 & 15800 & 16000 \\ 0.0035 & 0.0070 & 0.0105 & 0.0140 & 0.0175 \\ 0.0175 & 0.0349 & 0.0524 & 0.0698 & 0.0873 \\ 0.6000 & 0.7000 & 0.8000 & 0.9000 & 1.000 \\ 112000 & 114000 & 116000 & 118000 & 120000 \end{bmatrix}. \tag{39}$$

Example 1 (the failure-free simulation analysis between ATSM and FTC). In the example, the parameters of

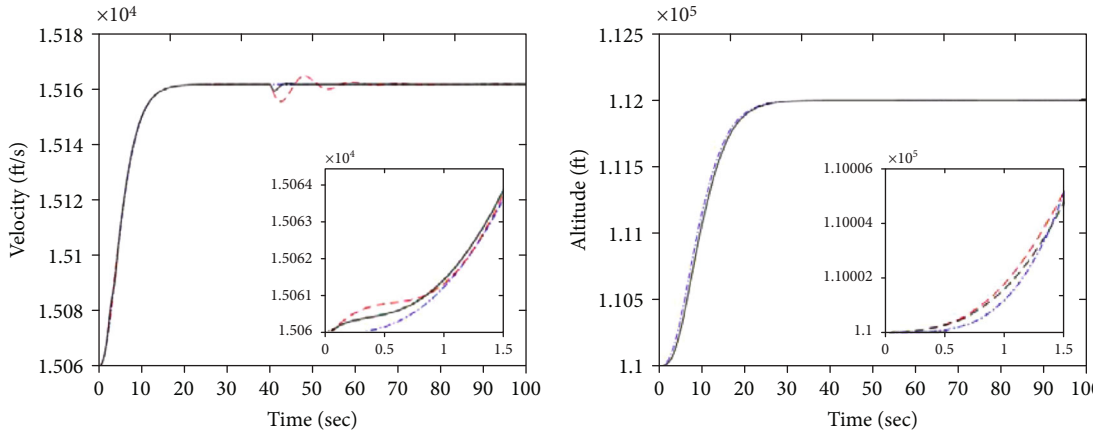

(a) Velocity

(b) Altitude

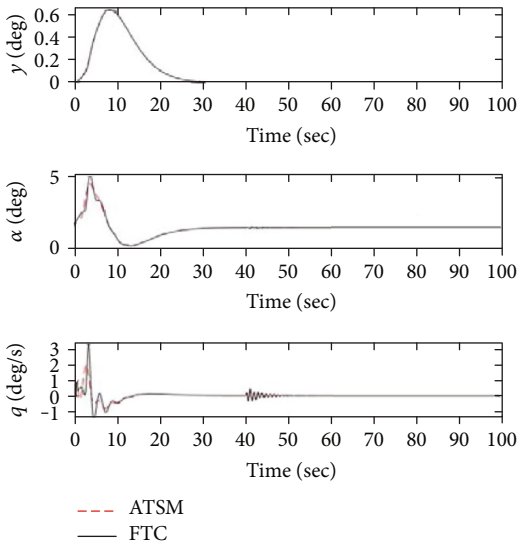

(c) Flight path angle, attack angle, and pitch rate

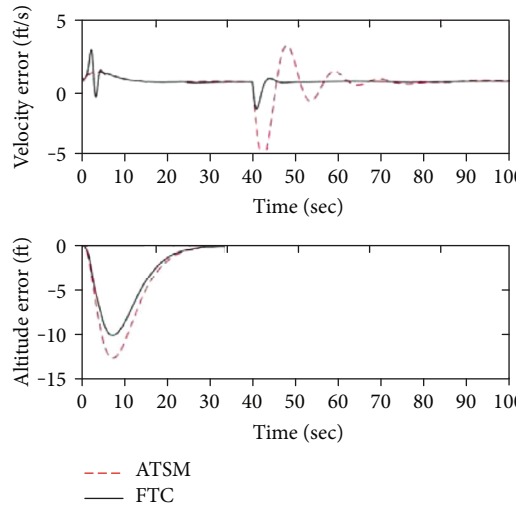

(d) Velocity error and altitude error

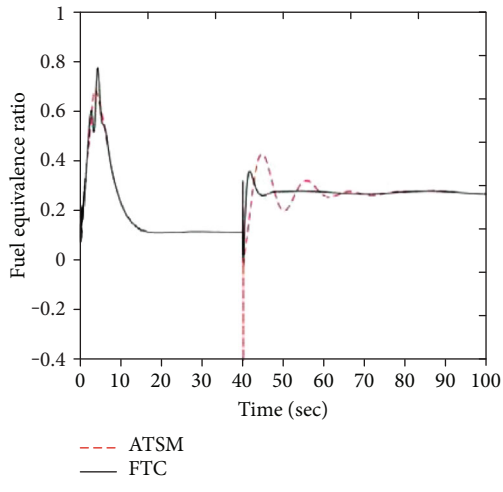

(e) Fuel-to-air ratio

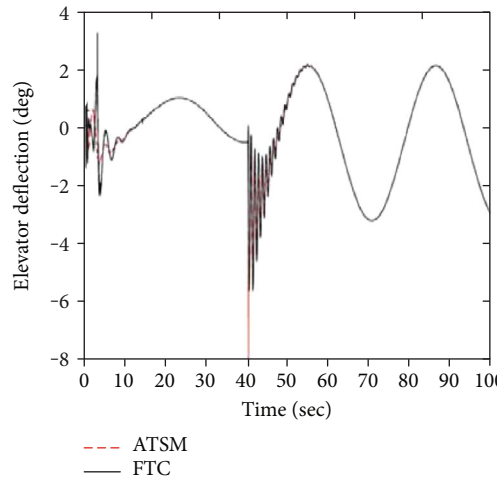

(f) Elevator deflection

Figure 3: Continued.

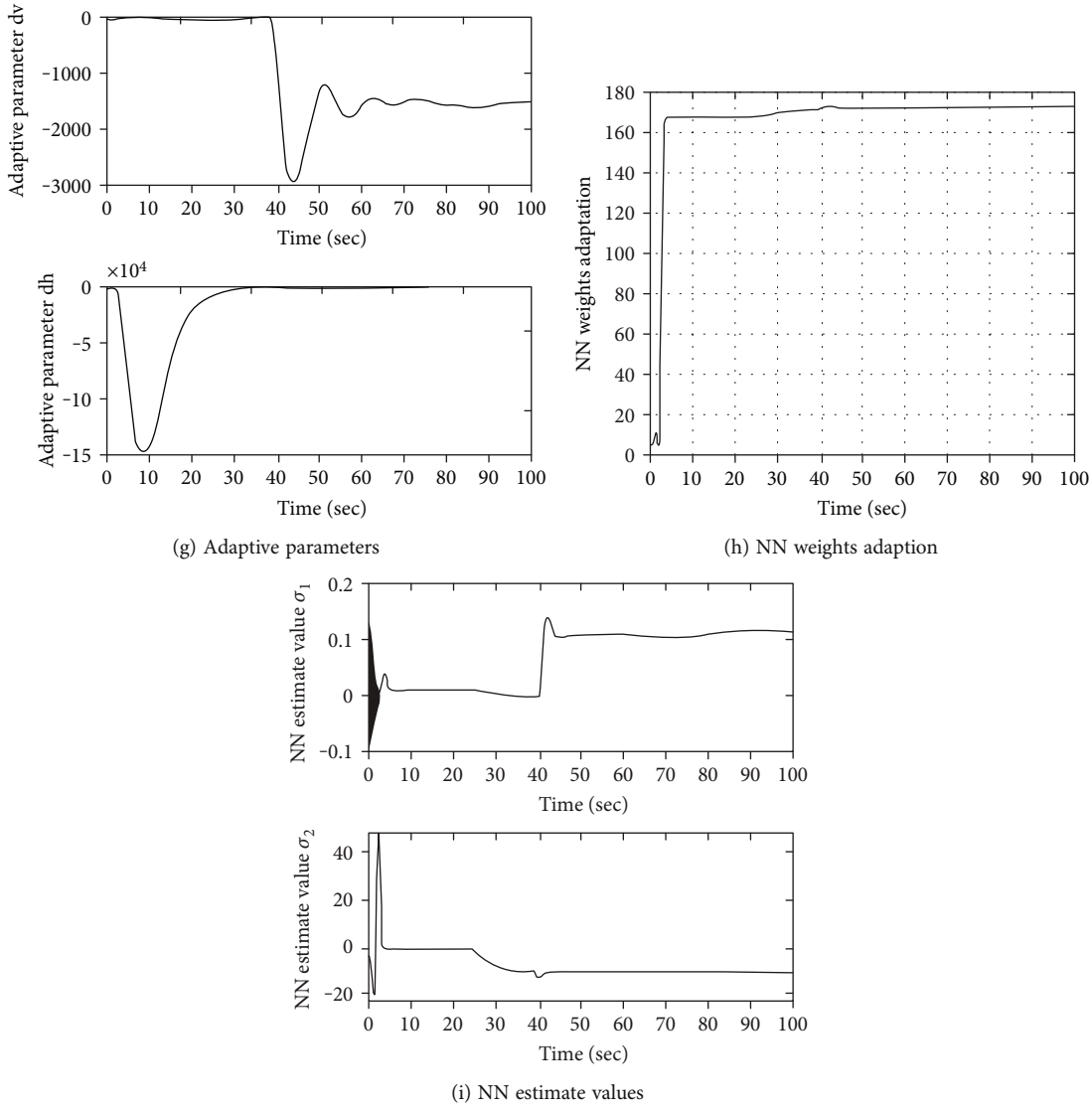

(g) Adaptive parameters

(h) NN weights adaption

(i) NN estimate values

Figure 3: The response curves of the ABHV's variables under the actuator faults.

Equation (5) are set as $k_F = 0$ and $d_F = 0$. The range of control input is set as $0 \le \phi_c \le 1$ and $-30 \le \delta_e \le 30(\text{deg})$. The simulation results are shown in Figure 2.

The tracking curves of velocity and altitude can be obtained from Figures 2(a) and 2(b), allowing the ATSM controller to track the reference command with a small tracking error. It is visible from Figures 2(a)–2(c) that the states converge to steady-state values in a brief period. Figures 2(d) and 2(e) show the control inputs of fuel-to-air ratio and deflection in the limit range, which are smooth. Figure 2(f) describes the curves of the adaptive parameters in the case of unknown uncertainties. The NN weight adaption and estimate values fluctuate quickly owing to tracking errors, as seen in Figures 2(g) and 2(h), and the variables converge to a constant in a limited amount of time.

Example 2 (the failure-tolerant simulation analysis between ATSM and FTC). In the example, the range of control input is set as in Example 1, and the parameters of Equation (5) are set as follows:

$$k_F(t) = \begin{cases} 0, & t < 40s, \\ [0.5 \quad 0.3]^T, & t \ge 40s, \end{cases}$$

$$d_F(t) = \begin{cases} 0, & t < 40s, \\ [0.001 \quad 0.001] * \sin\left(0.2t + \dfrac{\pi}{6}\right), & t \ge 40s. \end{cases} \tag{40}$$

The simulation results are shown in Figure 3.

The hypersonic vehicle is marginally impacted by velocity and altitude in time-varying fault conditions, as seen in Figures 3(a)–3(c). Figures 3(e) and 3(f) illustrate the curves of the input signal. From Figure 3(d), when simulating for 40 s, the actuator faults occur, the ATSM controller adjusts

the control gain rapidly, and the control input is out of the lower bound of the fuel-to-air ratio. The results of simulation show that the amplitude of deviation can be reduced with the method and improve the convergence of the states. From Figures 3(g)–3(i), it can be seen that the FTC scheme has a strong fault-tolerant capacity to adjust the adaptive parameters and the NN estimate values online and handle failure effectively under the occurrence of failure.

5. Conclusions

In this paper, the ABHV longitudinal model's parameter uncertainties, external disturbances, and actuator defects are investigated using radial basis function neural networks (RBFNN) and adaptive sliding mode (ATSM). The input-output linearization approach is used to create an adaptive terminal sliding mode controller based on the simplified nonlinear dynamics model of a hypersonic vehicle, which achieves speed and altitude tracking convergence in a short time. A fault-tolerant control (FTC) system was created to further tackle the actuator defect problem, and RBFNN was employed to simulate the unknown actuator dynamics. The Lyapunov theorem verifies the closed-loop system's uniformly ultimate stability. The FTC scheme is numerically simulated. The analysis and simulation findings reveal that the fault-tolerant control system described in this study can provide quick tracking response and has high resilience in the presence of actuator faults.

Data Availability

The model parameters of the numerical simulation used to support the findings of this study have been deposited in the "Design of robust control systems for a hypersonic aircraft" repository (doi:10.2514/2.4197).

Conflicts of Interest

The authors declare that they have no conflicts of interest.

Acknowledgments

This research was supported by the National Natural Science Foundation of China (No. 12072090).

References

[1] M. A. Bolender and D. B. Doman, "A non-linear model for the longitudinal dynamics of a hypersonic air-breathing vehicle," in *AIAA Guidance, Navigation, and Control Conference and Exhibit*, San Francisco, California, August 2005.

[2] C. I. Marrison and R. F. Stengel, "Design of robust control systems for a hypersonic aircraft," *Journal of Guidance, Control, and Dynamics*, vol. 21, no. 1, pp. 58–63, 1998.

[3] Q. Wang and R. F. Stengel, "Robust nonlinear control of a hypersonic aircraft," *Journal of Guidance, Control, and Dynamics*, vol. 23, no. 4, pp. 577–585, 2000.

[4] L. Wen, G. Tao, H. Yang, and B. Jiang, "Adaptive actuator failure compensation for possibly nonminimum-phase systems using control separation based lq design," *IEEE Transactions on Automatic Control*, vol. 64, no. 1, pp. 143–158, 2018.

[5] H. Y. Qiao, H. Meng, M. J. Wang, W. Ke, and J. G. Sun, "Adaptive control for hypersonic vehicle with input saturation and state constraints," *Aerospace Science and Technology*, vol. 84, pp. 107–119, 2019.

[6] B. Xu, X. Huang, D. Wang, and F. Sun, "Dynamic surface control of constrained hypersonic flight models with parameter estimation and actuator compensation," *Asian Journal of Control*, vol. 16, no. 1, pp. 162–174, 2014.

[7] S. Saki, H. Bolandi, and K. E. D. M. Mashhadi, "Optimal direct adaptive soft switching multi-model predictive control using the gap metric for spacecraft attitude control in a wide range of operating points," *Aerospace Science and Technology*, vol. 77, pp. 235–243, 2018.

[8] Y. Wang and Q. Wu, "Adaptive non-affine control for the short-period model of a generic hypersonic flight vehicle," *Aerospace Science and Technology*, vol. 66, pp. 193–202, 2017.

[9] H. Li, L. Wu, H. Gao, X. Hu, and Y. Si, "Reference output tracking control for a flexible air-breathing hypersonic vehicle via output feedback," *Optimal Control Applications & Methods*, vol. 33, no. 4, pp. 461–487, 2012.

[10] H. Xu, P. A. Ioannou, and M. Mirmirani, "Adaptive sliding mode control design for a hypersonic flight vehicle," *Journal of Guidance Control and Dynamics*, vol. 27, no. 5, pp. 829–838, 2004.

[11] H. Sun, S. Li, and C. Sun, "Finite time integral sliding mode control of hypersonic vehicles," *Nonlinear Dynamics*, vol. 73, no. 1-2, pp. 229–244, 2013.

[12] Y. Ding, X. Wang, Y. Bai, and N. Cui, "Global smooth sliding mode controller for flexible air-breathing hypersonic vehicle with actuator faults," *Aerospace Science and Technology*, vol. 92, pp. 563–578, 2019.

[13] J. G. Sun, S. M. Song, and G. Q. Wu, "Fault-tolerant track control of hypersonic vehicle based on fast terminal sliding mode," *Journal of Spacecraft & Rockets*, vol. 54, no. 6, pp. 1304–1316, 2017.

[14] L. Peng, "The design of fixed-time observer and finite-time fault-tolerant control for hypersonic gliding vehicles," *IEEE Transactions on Industrial Electronics*, vol. 65, no. 5, pp. 4135–4144, 2018.

[15] S. Ran, J. Wang, D. Zhang, and X. Shao, "Neural-network-based sliding-mode adaptive control for spacecraft formation using aerodynamic forces," *Journal of Guidance Control and Dynamics*, vol. 41, no. 3, pp. 1–7, 2017.

[16] C. Mu, N. Zhen, C. Sun, and H. He, "Air-breathing hypersonic vehicle tracking control based on adaptive dynamic programming," *IEEE Transactions on Neural Networks & Learning Systems*, vol. 28, no. 3, pp. 584–598, 2017.

[17] B. Xu, "Robust adaptive neural control of flexible hypersonic flight vehicle with dead-zone input nonlinearity," *Nonlinear Dynamics*, vol. 80, no. 3, pp. 1509–1520, 2015.

[18] Y. Meng, B. Jiang, and R. Qi, "Adaptive fault-tolerant attitude tracking control of hypersonic vehicle subject to unexpected centroid-shift and state constraints," *Aerospace Science and Technology*, vol. 95, article 105515, 2019.

[19] C. Luo, H. Lei, J. Li, and C. Zhou, "A new adaptive neural control scheme for hypersonic vehicle with actuators multiple constraints," *Nonlinear Dynamics*, vol. 100, no. 4, pp. 3529–3553, 2020.

[20] B. Xu, C. Yang, and Y. Pan, "Global neural dynamic surface tracking control of strict-feedback systems with application to hypersonic flight vehicle," *IEEE Transactions on Neural Networks & Learning Systems*, vol. 26, no. 10, pp. 2563–2575, 2017.

[21] X. Bu, Y. Xiao, and H. Lei, "An adaptive critic design-based fuzzy neural controller for hypersonic vehicles: predefined behavioral nonaffine control," *IEEE/ASME Transactions on Mechatronics*, vol. 24, no. 4, pp. 1871–1881, 2019.

[22] R. Xia, M. Chen, Q. Wu, and Y. Wang, "Neural network based integral sliding mode optimal flight control of near space hypersonic vehicle," *Neurocomputing*, vol. 379, pp. 41–52, 2020.

[23] A. Hao, Q. Wu, C. Wang, and X. Cao, "Scramjet operation guaranteed longitudinal control of air-breathing hypersonic vehicles," *IEEE/ASME Transactions on Mechatronics*, vol. 25, no. 6, pp. 2587–2598, 2020.

[24] H. An, Q. Wu, G. Wang, Y. Kao, and C. Wang, "Adaptive compound control of air-breathing hypersonic vehicles," *IEEE Transactions on Aerospace and Electronic Systems*, vol. 56, no. 6, pp. 4519–4532, 2020.

[25] R. Zhang, Q. Chen, and H. Guo, "Chebyshev neural network-based adaptive nonsingular terminal sliding mode control for hypersonic vehicles," *Mathematical Problems in Engineering*, vol. 2020, Article ID 6830141, 10 pages, 2020.

[26] D. Duan, L. Chu, and Y. Han, "Multi-dimensional Taylor network-based adaptive funnel tracking control of a class of nonlinear systems with prescribed performance," *IEEE Access*, vol. 8, pp. 132265–132272, 2020.

[27] B. Xu, Y. Shou, J. Luo, H. Pu, and Z. Shi, "Neural learning control of strict-feedback systems using disturbance observer," *IEEE Transactions on Neural Networks and Learning Systems*, vol. 30, no. 5, pp. 1296–1307, 2019.

[28] X. Zhang, K. Chen, W. Fu, and H. Huang, "Neural network-based stochastic adaptive attitude control for generic hypersonic vehicles with full state constraints," *Neurocomputing*, vol. 351, pp. 228–239, 2019.

[29] K. Sachan and R. Padhi, "Nonlinear robust neuro-adaptive flight control for hypersonic vehicles with state constraints," *Control Engineering Practice*, vol. 102, article 104526, 2020.